We are IntechOpen, the world's leading publisher of Open Access books
Built by scientists, for scientists

4,800
Open access books available

122,000
International authors and editors

135M
Downloads

Our authors are among the

154
Countries delivered to

TOP 1%
most cited scientists

12.2%
Contributors from top 500 universities

CLARIVATE ANALYTICS
BOOK CITATION INDEX
INDEXED

WEB OF SCIENCE™

Selection of our books indexed in the Book Citation Index in Web of Science™ Core Collection (BKCI)

Interested in publishing with us?
Contact book.department@intechopen.com

Numbers displayed above are based on latest data collected.
For more information visit www.intechopen.com

Chapter 1

High Volumetric Performance Supercapacitors with Controlled Nanomorphology

Yue Zhou and Qiming Zhang

Additional information is available at the end of the chapter

http://dx.doi.org/10.5772/65186

Abstract

Supercapacitor is one of the promising energy storage devices due to its relatively higher energy density compared with dielectric capacitor and higher power density and longer cycle life time (>millions) than conventional battery. In order to satisfy various requirements for energy technologies, supercapacitors with higher energy and power densities are required. In this chapter, we improved the electrochemical performance largely compared with commercial product through controlling the nanomorphology of cells. Meanwhile, although many past research programs have focused mainly on gravimetric energy densities, here we have also devoted efforts to study and develop nanomorphologic structures to realize high volumetric energy and power densities, since device volume is another critical and key performance parameter. Moreover, fundamental studies have been carried out on the mobile ion transport and storage in the nanostructures developed in this chapter.

Keywords: supercapacitor, carbon nanotubes, graphene, volumetric performance, nanomorphology control

1. Introduction

In order to meet different application requirements and also for fundamental studies of ion transport and storage in nanoporous media, we selected carbon-based electrodes with unique and controlled nanomorphologies: highly aligned carbon nanotube (A-CNT) forests. As synthesized, A-CNTs have low volume fraction of CNT (~1%). Traditional method to achieve high volumetric performance of A-CNTs was to employ liquid surface tension densification, which did not have control on the nanomorphology of A-CNTs after densification. In this

INTECH
open science | open minds

© 2016 The Author(s). Licensee InTech. This chapter is distributed under the terms of the Creative Commons Attribution License (http://creativecommons.org/licenses/by/3.0), which permits unrestricted use, distribution, and reproduction in any medium, provided the original work is properly cited. CC BY

work, making use of and improving upon the mechanical densification method, we achieved 40% volumetric density of A-CNTs. A series of supercapacitor electrodes have been developed and characterized. As can be seen in the section, the high volume fraction of A-CNTs and highly aligned ion channels in the nanoporous electrodes lead to the superior performance of the supercapacitors compared with any CNT-based supercapacitor electrodes studied earlier. The supercapacitors exhibit a volumetric power density, 25 kW/L (and gravimetric power density 50 kW/kg) for the capacitor cell with 0.8-mm thick A-CNTs, compared with the similar capacitors using A-CNTs densified by the liquid collapsing method, 13.4 kW/L (24 kW/kg) for cells with 0.5-mm thick A-CNTs. The study also shows the importance of the ionic conductivity of electrolytes in controlling the power and energy densities of the supercapacitors.

Since the energy and power densities of supercapacitors are directly proportional to the square of cell operation voltage V (~ V^2), raising the cell operation voltage will have great potential to enhance the energy and power densities. Asymmetric supercapacitors, which allow for optimization of both cathode and anode simultaneously, provide an attractive approach to raise the cell operation voltage, besides other properties. In this chapter, we have investigated asymmetric supercapacitor configurations for carbon-based electrodes for one electrode and conducting polymer (CP)-coated A-CNTs for the other one, based on their electrochemical windows. Here, we investigate the asymmetric supercapacitors where both electrodes are tailored, respectively, to improve the device electrochemical performances such as specific capacitance and the electrochemical window. Hence, operating voltage is increased. The conformal vapor is utilized to deposit CP on the A-CNTs, enhancing the charge storage capability of the electrode, while the aligned nanowire morphology of the composite electrode exhibits straight fast ion transport pathways to enhance power. The a-graphene electrode, which is fabricated through a self-assembly process, shows the high active material density. Combining with a high specific surface area of 3000 m^2/g, the electrode yields very high specific volumetric capacitance, energy, and power densities. As a result, the asymmetric supercapacitors show an energy density 113 Wh/L (176 Wh/kg), which is the highest among all carbon-based supercapacitors, and a power density 149 kW/L (233 kW/kg).

2. Symmetric supercapacitors with controlled unique nanomorphology

Presently, most supercapacitors are fabricated from activated carbon (AC), which possesses a very large specific surface area (1000–2000 m^2/g). Recent advances have demonstrated many attractive features of utilizing A-CNTs for supercapacitors with nanoporous electrodes, especially the parallel ion channels formed by the A-CNTs that improve the ion transport, as schematically illustrated in **Figure 1(a)**, compared with randomly arranged nanoporous electrodes from AC, forming tortuous ion transport pathways [1, 2]. Consequently, supercapacitor cells with A-CNTs exhibit higher power and energy density than that from AC. Since as grown A-CNT forests have CNT volumetric density <5 vol%, A-CNTs should be densified to reach higher A-CNT volumetric density for practical supercapacitor applications. In the past decade, many works have been conducted to produce

http://dx.doi.org/10.5772/65186

aligned A-CNTs with high CNT density to achieve high volumetric capacitance, energy density, and power density, which are critical for modern electric and electronic systems to realize compact device size and increased functions within given device volumes. For example, Futaba et al. [3] employed a liquid collapsing method to densify A-CNTs with a high density (~50 vol%). Here, the mechanical densification method has several advantages compared with the liquid collapsing method. This method provides a precise control on the density of the final A-CNTs, ranging from the original 1 vol% A-CNTs to >50 vol%. Besides, A-CNT samples with different sizes can be densified with precisely controlled nanomorphology (alignment), and hence this method provides a realistic pathway for scaling up high-density A-CNTs for large-scale manufacturing of supercapacitors from A-CNTs of ultrahigh volume density [4]. In addition, the availability of A-CNTs with different density and hence different ion channel sizes also creates a great opportunity to study how the ion channel size formed by the A-CNTs affect ion transport and storage, which is of great importance in developing supercapacitors with high energy, power density, and tailored performance. We have also studied the influence of the ionic conductivity of electrolyte on the electrochemical performance of the supercapacitors. An imidazolium-based ionic liquid (1-ethyl-3-methylimidazolium-tetrafluoroborate, EMI-BF_4) was chosen for the study. Imidazolium ionic liquids (ILs) due to their high ionic conductivity and wide elec-

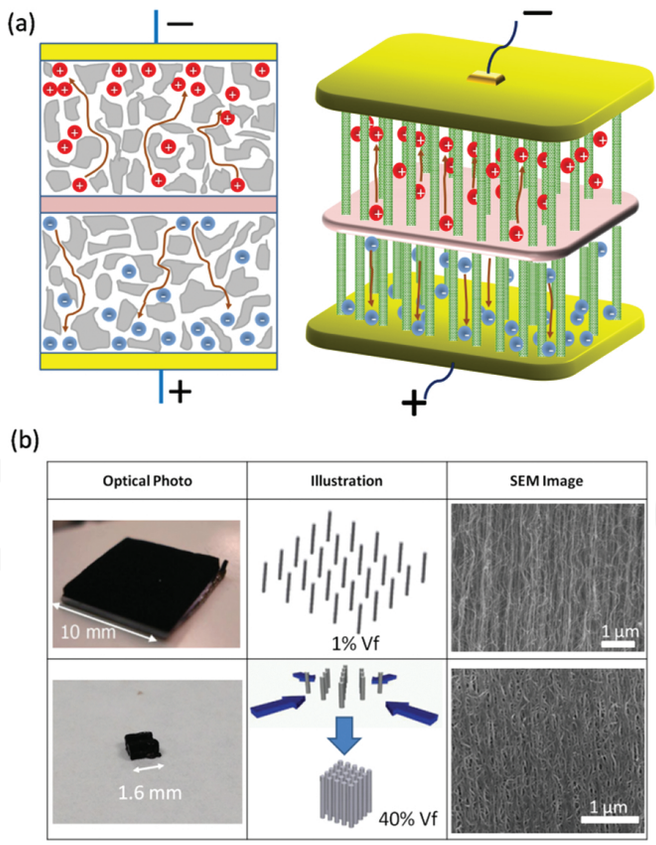

Figure 1. (a) The illustration of the tortuous ion transport paths in the activated carbon electrodes as well as parallel ion pathways in the A-CNTs. (b) Optic images, mechanical densification process, and SEM images of 1% Vf and 40% Vf A-CNTs.

trochemical window have been investigated very extensively as the electrolytes for supercapacitors. A mixture of an IL such as EMI-BF_4 and molecular liquid such as propylene carbonate (PC) can lead to marked enhancement (more than two times higher) in the ionic conductivity compared with the pure EMI-BF_4. The experimental results show that increased ionic conductivity of the electrolyte can lead to a large increase in the power density (more than double the power density using EMI-BF_4/PC compared with pure EMI-BF_4) of the supercapacitors.

The A-CNTs in this work were fabricated through a modified chemical vapor deposition (CVD) method on silicon wafers and iron (Fe) on alumina was used as the catalyst. The as-grown carbon nanotube forests have a 1% volume fraction (Vf) with density of 10^9–10^{10} CNTs cm^{-2}. The average diameter of nanotubes is 8 nm with 3–5 multiwalls. The spacing between nanotubes is approximately 80 nm in the forest. For the high Vf A-CNT synthesis, the freestanding CNT forests were released from the silicon wafer using a razor blade. And then as shown in **Figure 1(b)**, the forests were subjected to a mechanical biaxial densification process in two orthogonal directions. In this method, the A-CNT forest was densified along one direction firstly to a fixed distance by utilizing a mechanical bar, and then another mechanical bar in the orthogonal direction was employed to compress the A-CNT forest to the final volume fraction. By varying the inter-CNT distance in densification process, A-CNT forests with different Vfs can be obtained.

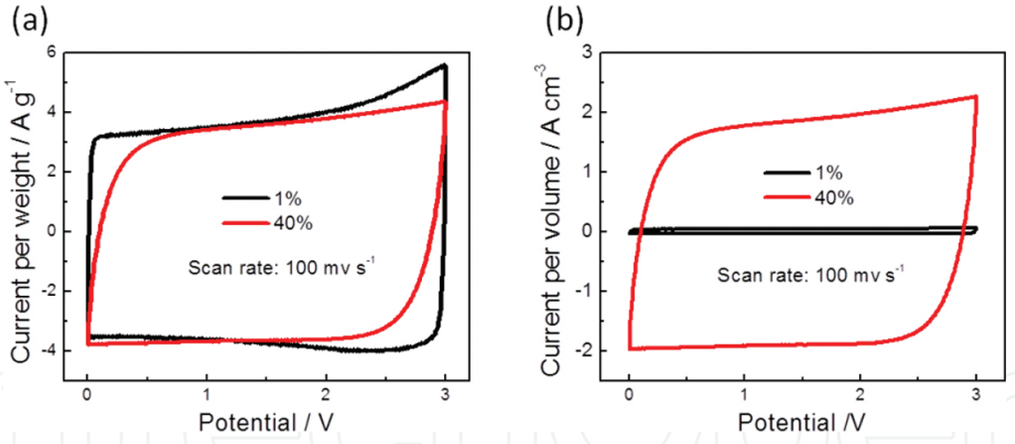

Figure 2. Electrochemical performance of supercapacitors with A-CNT electrodes and EMI-BF4/PC electrolyte at 4 V: (a) gravimetric cyclic voltammograms and (b) volumetric cyclic voltammograms of A-CNT electrodes with 1% and 40% Vf at 100 mV s^{-1}.

The A-CNT forests were used as the electrodes of the supercapacitors. 3 M EMI-BF_4 (1-ethyl-3-methylimidazolium tetrafluoroborate) in propylene carbonate (PC) was used as the electrolyte to improve ionic conductivity. Compared with pure ionic liquid, the ionic liquids/molecular liquids (IL/ML) mixture will have higher conductivity. Polypropylene porous membrane (Celgard 3501, Celgrad LLC) with 25 μm thickness was used as the separator. The sandwich architecture (electrode/separator/electrode) was placed between two pieces of Au-coated steel plates, which served as the current collectors. Then, the whole cell was housed in a Teflon

holder. As a comparison, supercapacitor electrodes, which are made from the activated carbon powders mixing with 10 wt% PTFE and 10 wt% carbon black, were also fabricated using the standard method.

Figure 2(a) presents the cyclic voltammetry (CV) curves at 100 mV s^{-1} scan rate of supercapacitors with 1% Vf and 40% Vf of A-CNTs as electrodes in 3 M EMI-BF_4/PC electrolyte. As shown in the figure, there is very little difference in the gravimetric capacitance drop as the A-CNT Vf increases from 1% to 40%, showing that the densification process can still maintains the aligned nanomorphology with parallel ion pathways. On the other hand, increasing the A-CNT Vf from 1% to 40% leads to a large increase considering the volumetric capacitance performance, as shown in **Figure 2(b)**.

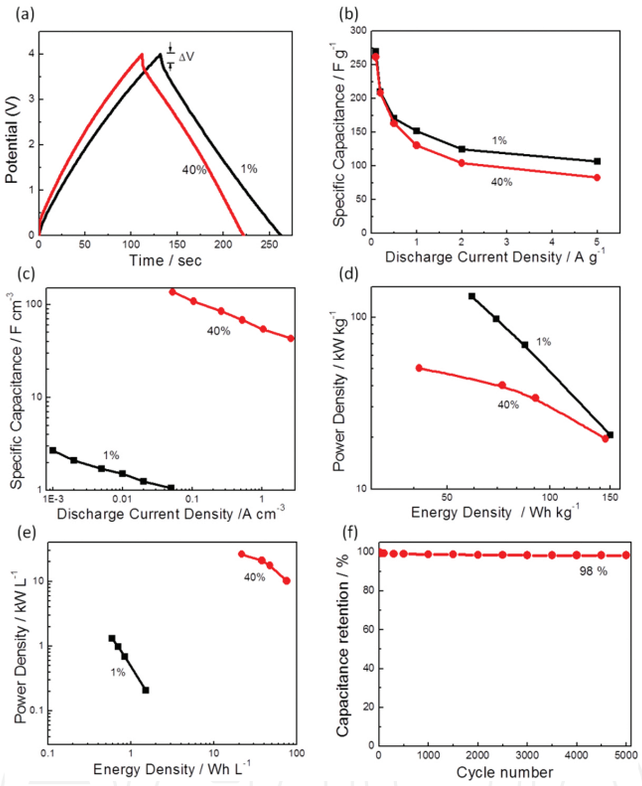

Figure 3. (a) Galvanostatic charge and discharge curves at 1 A g^{-1} for supercapacitors with electrodes of 1% and 40% Vf forests and EMI-BF4/PC as electrolyte. (b) Gravimetric and (c) volumetric specific capacitances for the supercapacitors with electrodes of 1% and 40% Vf forests with different discharge rates. (d) Gravimetric and (e) volumetric Ragone plots for the supercapacitors with electrodes of 1% and 40% Vf A-CNTs. (f) Cycle retention performance of 40% Vf A-CNT supercapacitor with a voltage of 4 V under the charge and discharge current density of 5 A g^{-1}.

The galvanostatic cycles between 0 and 4 V for the supercapacitors with 1% Vf and 40% VfA-CNT electrodes under 1 A g^{-1} current density are presented in **Figure 3(a)**. The capacitance of the cell can be determined:

$$C = I / \left(dV / dt \right) \tag{1}$$

where I is the constant current density, V is potential, and t is discharge time. **Figure 3(b)** and **3(c)** shows the specific gravimetric and volumetric capacitances with different discharge currents, respectively. Although the cell with electrodes of 1% Vf show a little higher specific gravimetric capacitance which is larger than 270 F g^{-1}, their volumetric capacitance is very low (around 3 F cm^{-3}).

It should be mentioned that the 1% Vf A-CNT electrode has a very low active material density with 0.013 g/cm^3. For this kind of electrode, the majority of the electrode volume is filled with electrolytes, whose mass is not included when evaluating the gravimetric electrochemical performance. Instead, the volumetric values should be utilized to investigate when comparing electrodes with large difference about the active material density. It could be found that the specific volumetric capacitance of 40% Vf A-CNT electrodes is about 40 times higher than that of 1% Vf A-CNT electrodes, exhibiting that the nanomorphology of the A-CNTs is preserved by utilizing the mechanical densification method developed here.

The maximum power density and energy density of the supercapacitor cells can be calculated based on the equivalent series resistance (ESR) and the specific capacitance. The gravimetric and volumetric Ragone plots for the supercapacitor cells are shown in **Figure 3(d)** and **3(e)**, respectively. The energy of the supercapacitor cell under each discharge current can be calculated by integrating the discharge curves with time.

$$E = \int IV(t)dt \tag{2}$$

The ESR can be calculated based on the equation below:

$$ESR = \Delta V / \Delta I \tag{3}$$

where ΔV is the voltage drop as the current is switched from a positive value to a negative value, such as from 1 Ag^{-1} to −1 Ag^{-1} ($\Delta I = 2$ Ag^{-1}). The maximum power density, hence, can be deduced from:

$$P = V^2 / (4 \times ESR) \tag{4}$$

The active material density of the electrodes in many recently developed nanoporous electrodes, such as the A-CNT electrodes described here, can vary over a broad range. The traditional method to evaluate the performance of supercapacitor cell such as the gravimetric energy and power densities will not accurately reflect the device performance because the only mass of the conductive electrode material is included and the active material density is usually very low. For example, due to a very large "empty space" (80 nm between nanotubes) in the ion pathway, a very high power density of 100 kW kg^{-1} was obtained in the supercapacitor cell with 1% Vf A-CNT forests as the cell electrodes. As a comparison, 50 kW kg^{-1} was obtained in the supercapacitor cell based on 40% Vf A-CNT forests as electrodes due to the smaller pore

size. However, the supercapacitor cell with 1% Vf A-CNT forests shows a very low gravimetric maximum power and energy density compared with that of the supercapacitor cell based on 40% Vf A-CNT forests if the total electrode mass, including all the elements such as the active materials and the electrolytes, is considered.

For the supercapacitor cells with 1% Vf of A-CNT forests as electrodes, the specific gravimetric capacitance will decrease to 4.3 Fg^{-1} when the total electrode mass, including both the 1% Vf active material (A-CNTs) and 99% Vf electrolyte, is used for the calculation. This is much smaller than 270 F g^{-1} calculated when only the mass of the A-CNTs is included. In contrast, for the 40% Vf A-CNTs, a gravimetric capacitance of 270 F g^{-1} for the active material alone is equivalent to a 139.8 F g^{-1} when all the electrode mass is included.

The supercapacitors based on 40% Vf A-CNTs also exhibit an excellent cycling life as shown in **Figure 3(f)**. The data were acquired over 5000 cycles by repeating the galvanostatic charge and discharge process between 0 and 4 V under an alternate current densities of 5 and −5 A g^{-1}, which show an excellent electrochemical stability. Capacitance retention of 98% after 5000 cycles was obtained based on the supercapacitor cell with the ultra-high density A-CNTs as 40% Vf.

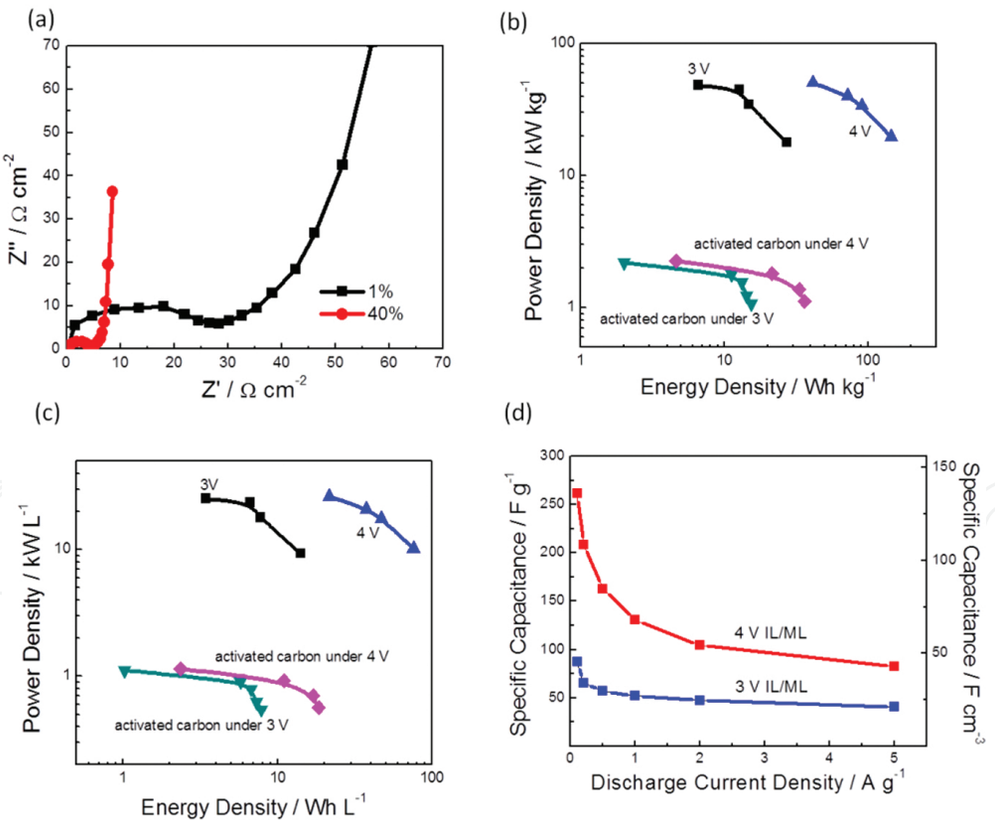

Figure 4. (a) Nyquist plots of supercapacitors based on A-CNTs with the two volume fractions in the range of 100 kHz to 10 mHz. (b) Gravimetric and (c) volumetric Ragone plots of supercapacitor cells with electrodes based on 40% Vf A-CNT forests and with electrodes using activated carbon. (d) Under several discharge current densities, the relationship of specific capacitance of cells based on 40%Vf A-CNT forests.

The electrochemical impedance spectroscopy (EIS) analysis was carried out to investigate the possible influence of the ultra-high density A-CNT forests on the electrochemical performance of supercapacitor electrodes. **Figure 4(a)** shows the EIS figure in the frequency range of 100 kHz–10 mHz. The Nyquist plots of supercapacitor cells with electrodes based on 1% and 40% Vf A-CNT forests show both semicircles in the high/middle frequency and sharp rises at low frequency range. The semicircle behavior is due to the charge transfer resistance of the electrodes, and the sharp increase at low frequency range is resulted from the ideal capacitive performance of the electrode. It could be found that the cell with electrodes based on 40% Vf A-CNT forests also show much smaller resistance (Z′) when normalized with the area of the capacitors (Ω cm^{-2}) compared with that of electrodes based on 1% Vf A-CNT forests.

As a comparison, activated carbon with the thickness of 800 μm was fabricated. The maximum power density, energy density, and electrochemical performances of cells based on activated carbon are shown in **Figure 4(b)** and **4(c)**. A much lower volumetric energy density and power density (20 and 1.1 kWL^{-1}, under 4 V) were obtained based on the activated carbon electrodes, compared with the performance with 40% Vf of A-CNT forests (75 and >25 kW L^{-1} under 4 V). These results indicate the superior electrochemical performance of the ultra-high-density A-CNT electrodes fabricated from the mechanical densification method developed here. The nanomorphology of the aligned ion pathways leads to the fast charge/discharge rate and high power/energy densities.

Figure 4(b) and **4(c)** presents that there is very little increase in the power density while increasing the voltage from 3 to 4 V leads to a large increase in the energy density, from 15 to 75 Wh L^{-1} (gravimetric 30–150 Wh kg^{-1}). The large increase in the energy density results from the increase in the specific capacitance of the electrodes with the increasing of voltage, as shown in **Figure 4(d)**. The specific capacitance is obtained as 260 F g^{-1} (135 F cm^{-3}) at 4 V. These values are much higher than those reported earlier for the supercapacitors utilizing densified A-CNTs through the liquid collapsing method. On the other hand, it is noted that the maximum power density depends on the ESR (see Equation (4)), as well as the applied voltage. The results exhibit that there is a large increase in the ESR as the operation voltage has increased from 3 to 4 V, which is consistent with the results of an earlier study in our group [5]. Diffusion process and drifting process have dominated the transport of mobile ion in ionic devices such as supercapacitors. Diffusion is relatively slower and hence represents much higher ESR compared with drifting process.

3. Asymmetric supercapacitor with high electrochemical performance

In this work, an asymmetric supercapacitor, exploiting nm-scale conformal coating of a conducting polymer, poly(ethylenedioxythiophene) (PEDOT) on aligned carbon nanotubes (A-CNTs) as one electrode and an ultra-high density aligned graphene sheets (a-graphene) as the other electrode, has been developed. The asymmetric configuration of the supercapacitor allows both electrodes to be separately tailored, increasing device capacitance and the electrochemical window, and thereby operating voltage. As a result of complementary

http://dx.doi.org/10.5772/65186

three-dimensional nanotailoring of the asymmetric electrodes, the device exhibits a wide 4V electrochemical window and high electrochemical performance [6].

For supercapacitors, it is well known that the energy density (E) is related to the gravimetric or volumetric cell capacitance (C) and operation voltage (V), i.e.

$$E = \frac{1}{2}CV^2 \tag{5}$$

And the maximum power density P is determined by Equation (4). Equations (4) and (5) have shown that one of the most effective ways to increase both the power and energy densities is to raise the cell operation voltage. In general, the operation voltage of supercapacitor cell has the relationship with the electrochemical window, which is determined by the interface between the electrode and electrolyte. As a promising way, asymmetric supercapacitor can be assembled to make full use of the electrochemical windows of both electrodes to increase the maximum cell operation voltage in the supercapacitor cell. Morphology control of the electrodes via nanoscale tailoring is shown to be an effective way to increase supercapacitor performance (gravimetric and volumetric power and energy) via increasing ECW and capacitance and reducing ESR.

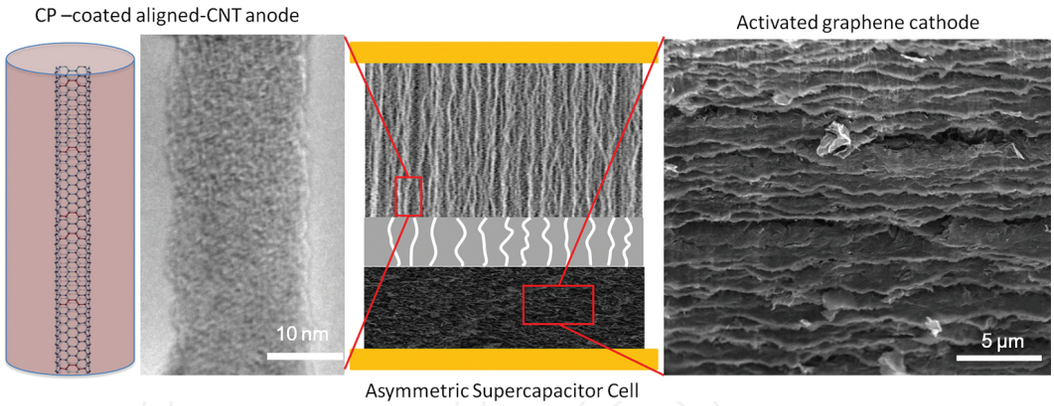

Figure 5. Nanostructured electrodes in asymmetric supercapacitors. Left, Low and high magnification TEM micrographs of the electrode, composed of conformal oCVD PEDOT on A-CNTs, and right, SEM images of activated graphene electrode.

Recent advances in the conformal coating of conducting polymer PEDOT by oxidative chemical vapor deposition (oCVD) onto nanowire arrays and development of graphene with relatively high gravimetric surface area create unique opportunities for developing high performance asymmetric supercapacitors. As schematically illustrated in **Figure 5**, the combination of the aligned ion transport pathways formed by the aligned nanowire arrays that provide fast ion transport in the electrode that reduces ESR of the electrode and the conformal coating of conducting polymer PEDOT on the A-CNTs that enhances the charge storage capability (a large C) contributes to both high energy and power densities of the cells. PEDOT was selected as the conducting polymer because of its environmental stability, high

electrical conductivity, and a wide ECW. As shown in **Figure 6(a)**, conformally coated oCVD PEDOT on the A-CNTs yields a stable ECW from −1.0 to 1.8 V, when using an ionic liquid/molecular liquid mixture, 2 M 1-butyl-3-methylimidazolium tetrafluoroborate (BMI BF_4)/propylene carbonate (PC), as the electrolyte. The high ECW of 1.8 V makes it as an excellent positive electrode material in the asymmetric supercapacitors.

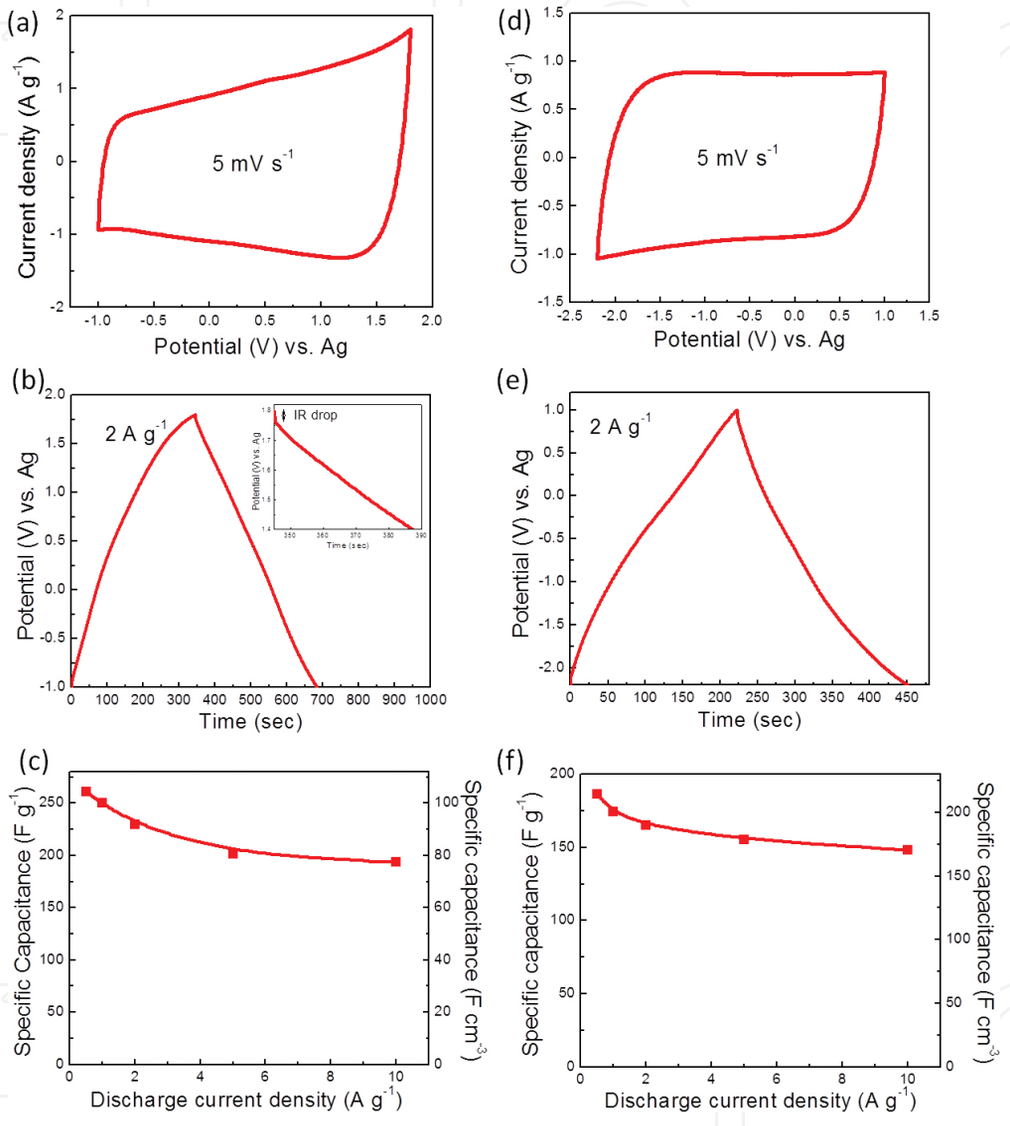

Figure 6. Performance of two electrodes: (a) CV curves of PEDOT/A-CNTs composite at 5 mV s^{-1} in 2 M BMIBF4/PC. (b) Galvanostatic charge/discharge curves of PEDOT/A-CNT composite at current densities of 2 A/g. (c) Specific capacitance at different discharge densities of PEDOT/A-CNT electrode. (d) CV curves of a-graphene at 5 mV/s in 2 M BMIBF4/PC. (e) Galvanostatic charge/discharge curves of a-graphene at current densities of 2 A/g. (f) Specific capacitance at different discharge densities of a-graphene electrode.

Due to their favorable ECWs, carbon-based electrodes such as activated carbon have been used for the negative in the asymmetric supercapacitors. In this study, a new class of carbon material, the a-graphene, was selected due to its superior gravimetric surface area compared with activated carbon. The a-graphene, first reported by Zhu et al., presented a very large specific

surface area (as large as 3100 m^2/g) with nanosized pores and demonstrated a gravimetric capacitance as high as 200 F/g when assembling supercapacitors [7]. However, the simple mechanical packing of the a-graphene flakes led to a relatively low density (~0.3 g/cm^3) compared with the graphite density of 2.2 g/cm^3. A low volumetric efficiency of supercapacitors was obtained by this configuration (the specific volumetric capacitance was 60 F/cm^3). When randomly packing these a-graphene flakes, which have lateral dimension of a few microns and a thickness of a few nanometers, it is inevitable to include micron-sized pores in the electrodes, reducing the density. Self-assembly processes are quite effective in increasing the density of graphene-based materials. Here, by employing a vacuum-assisted self-assembly process, which enabled a-graphene flakes aligned in parallel and stacked successively on top of each other, as shown by the SEM image of **Figure 5**, we fabricated the a-graphene electrodes with high density while preserving the nanoporous morphology of each a-graphene flake. The ECW of the a-graphene was also characterized, and as presented in **Figure 6(d)**, the a-graphene has a stable ECW from −2.2 V to 1 V with an electrolyte of 2M $BMIBF_4$/PC. The combination of high specific gravimetric surface area and high density of the a-graphenes as the negative electrode increases the ECW and results in high volumetric power and energy densities, besides the long cycle lifetime and high capacitive retention.

The high density (through packing) of aligned carbon nanotube (A-CNT) forests are distinctively advantageous as the conductive networks to support the CP coating layer in supercapacitors, when we compare with randomly packed morphologies. Besides the direct (and thereby fast) ion transport in aligned channel to reduce ESR illustrated in **Figure 5**, the PEDOT/A-CNT composite also provides better mechanical stability and hence higher retention property after many charge and discharge cycles, compared with the electrodes of the PEDOT/randomly packed CNT networks. In the extant literature, most electrodes of CP/CNTs were fabricated by electrochemical methods, which will lead to nonuniform CP layers coating on the CNTs. As shown in **Figure 6**, the thin (~5 to 10 nm) oxidative chemical vapor deposition (oCVD), PEDOT layers form a conformal coating on very high aspect ratio A-CNTs (0.2 mm long).

The electrochemical performance of PEDOT/A-CNT composite electrode were investigated by cyclic voltammetry (CV) and galvanostatic charge-discharge tests using a screen-printed electrode system (Dropsens) with the PEDOT/A-CNT composite as the working electrode, while Ag and Pt were employed as the reference and counter electrodes, respectively. **Figure 6(a)** shows a CV curve of the PEDOT/A-CNT forest composite electrode in 2 M $BMIBF_4$/PC electrolyte under a scan rate of 5 mV s^{-1}, which shows an ECW from −1 V to +1.8 V. The galvanostatic cycles for the PEDOT/A-CNT electrode at the alternate currents of 2 and −2A g^{-1} are shown in **Figure 6(b)**. The symmetric and linear charge and discharge characteristics with time reveal a rapid I-V response and reversible electrochemical reaction, leading to an superior capacitive behavior. The specific capacitance of the electrode can be determined from Equation (1). A high specific gravimetric capacitance of 230 F/g was obtained at 2 A/g. **Figure 6(c)** presents the specific capacitance at different discharge current density, from 0.5 to 10 A/g. Capacitance retention of 74.2% was obtained at 10 A/g (from 260.8 F/g at 0.5 A/g to 193.5 F/g at 10 A/g), indicating that the PEDOT/A-CNT electrode provide reliable capacitive

performance for high power applications. This relatively high retention mechanistically arises from the conformal coating of oCVD PEDOT on A-CNTs. The parallel ion transport pathways formed by the PEDOT/A-CNTs and the high electronic conductivity of the A-CNTs improve the ion transport and result in low ESR and therefore high power density. The cycling stability of the PEDOT/A-CNT electrodes was characterized and compared with that of the electrodes of PEDOT deposited on randomly packed CNT networks. Symmetric supercapacitors made of the PEDOT/A-CNTs had a retention of 89% after 1000 cycles of 2 V voltage cycle compared with a retention of 73% after 1000 cycles from PEDOT on random CNT morphologies. In the randomly packed CNT networks, there are CP layers in the gaps between nanotubes. The mechanical failure of CP layers in these gaps will cause disruption of the electric conduction paths between nanotubes and reduce the conductivity of CNT networks after long charge/discharge cycles. As a result, the capacitance and other electrochemical performances will be influenced. In contrast, the electric conduction path of the continuously aligned CNT forests would not be disrupted by the mechanical failure of the CP coating layers due to this nanomorphology. Hence, the A-PEDOT/A-CNT electrodes exhibit more robust mechanical stability and high retention of the capacitance, compared with the electrodes of the CP deposited on randomly packed CNT networks.

The electrochemical performance of the a-graphene electrode was characterized as above, including using 2 M $BMIBF_4$/PC as the electrolyte. **Figure 6(d)** presents a CV curve of the a-graphene electrode at a scan rate of 5 mV/s, showing an ECW of −2.2 V to +1 V. The slope of the discharge curve in **Figure 6(e)** yields a specific capacitance of 165 F/g at 2 A/g. The specific capacitances of the a-graphene electrode with different discharge currents are presented in **Figure 6(f)**. The a-graphene electrode exhibits high specific capacitance, ranging from 186.4 to 148.2 F/g as the discharge current increases from 0.5 A/g to 10 A/g. Moreover, the high density of the a-graphene electrodes results here in a specific volumetric capacitance with 175 F/cm^3 from the discharge curve of constant current of 1 A/g, which is the highest among all the carbon-based electrodes.

Both electrodes are independently tailored in asymmetric supercapacitors to operate under more optimal conditions. Here, the PEDOT/A-CNTs electrode and a-graphene electrode were assembled, separated by a porous paper of 40 μm thick. 2 M BMIBF4/PC was used as the electrolyte due to its high ionic conductivity. By properly tuning the mass ratio of the two electrodes, the asymmetric capacitor can be operated at the full 4 V cell operation voltage, reaching the maximum voltages from both electrodes (=1.8 V (A-CNT/PEDOT composite, V_+) + 2.2 V (a-graphene flakes, V_-)). Based on the consideration that charge stored at the two electrodes should be equal in magnitude with opposite sign ($|q_+| = |q_-|$), the mass ratio between the two electrodes can be determined as following equation if we consider the stored charge q at the electrode is $q = C\Delta Vm$, where C is the specific gravimetric capacitance, ΔV is the maximum potential range allowed by the ECW, and m is the mass of the electrode.

$$\frac{m_+}{m_-} = \frac{C_-\Delta V_-}{C_+\Delta V_+} \tag{6}$$

http://dx.doi.org/10.5772/65186

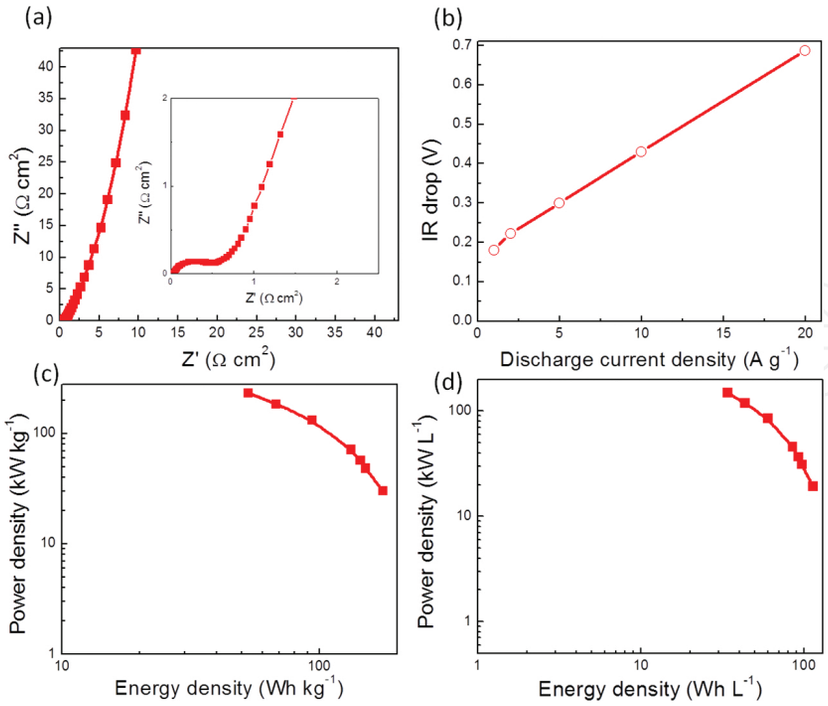

Figure 7. Cell performance: (a) CV curves of asymmetric cell under different scan rates from 5 to 100 mV/s between 0 and 4 V using 2 M BMIBF4/PC as the electrolyte. (b) Galvanostatic charge/discharge curves of asymmetric cell under a current density of 2 A/g. (c) Cell capacitances of asymmetric cell at different discharge current densities. (d) Cycle capacitance retention of asymmetric supercapacitor under a voltage of 4 V at a current density of 5 A/g in 2 M BMIBF4/PC electrolyte.

From the specific capacitances of the two electrodes, 230 and 165 F/g, respectively, under a constant discharge current of 2 A/g, and $\Delta V_+ = 1.8$ V and $\Delta V_- = -2.2$ V, Equation (6) can lead to the mass ratio (m_+/m_-) of 0.88, for a full 4 volts cell operation voltage, providing the design characteristics of the asymmetric supercapacitor assembled here.

Figure 7(a) presents the CV curves of the fabricated asymmetric supercapacitors at scan rates from 5 to 100 mV s^{-1} using the 2 M $BMIBF_4$/PC as electrolyte. The capacitors display near rectangular CV curves, especially for the lower scan rates. In order to evaluate the capacitive performance of the cell further, galvanostatic charge/discharge curves at different current densities were characterized. The galvanostatic cycles at alternate charge/discharge current densities of 2 and –2 A/g are presented in **Figure 7(b)**, from which the cell capacitance was determined (Equation (1)). **Figure 7(c)** presents the cell gravimetric and volumetric capacitances at different discharge currents. It should be noted that the calculated cell capacitance was based on the total mass of the active materials (both positive and negative electrodes) because it is not meaningful to deduce the specific capacitance of a single electrode for the asymmetric supercapacitor. The cell capacitance is 81.6 F/g at 0.2 A/g and becomes 55.4 F/g as the discharge current density increases to 10 A/g, indicating relatively good capacitance retention. The cell capacitance obtained here is higher than that of a-graphene-based symmetric supercapacitors and other conducting polymer-based asymmetric supercapacitors. Cycling retention performance of the asymmetric supercapacitors was investigated by continuously performing the

galvanostatic charge/discharge process between 0 and 4 V at the alternative current densities of 5 and −5 A/g for more than 1000 cycles. The asymmetric supercapacitor maintains electrochemical retention of 94% after 1000 cycles as presented in **Figure 7(d)**. The small capacitance loss is likely attributable to capacitance decay of the PEDOT/A-CNT electrode.

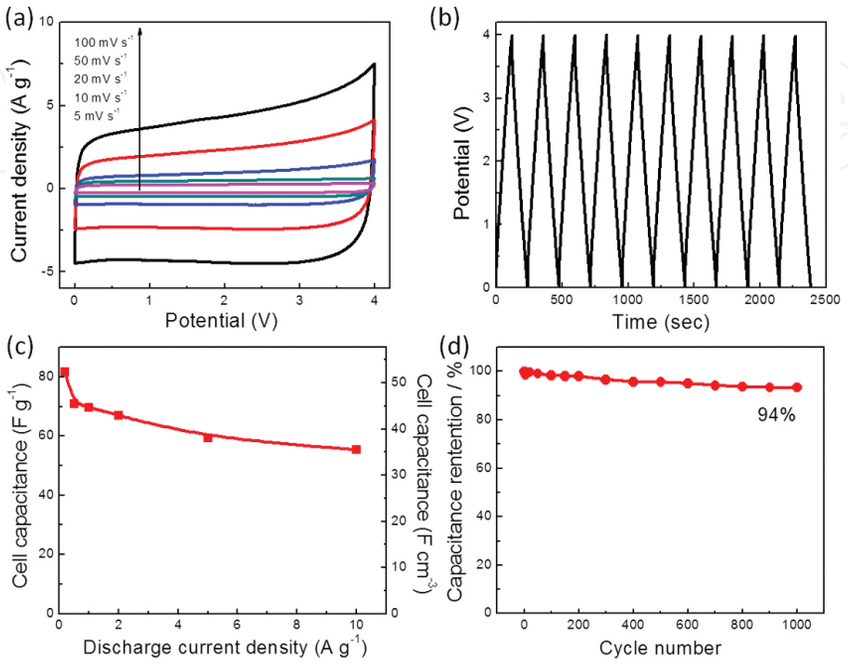

Figure 8. Asymmetric cell absolute and relative performance: (a) Nyquist plot of the asymmetric cell. (b) Internal resistance drop at different current densities. (c) Ragone plot of PEDOT/A-CNTs//a-graphene asymmetric supercapacitor in gravimetric unit. (d) Ragone plot of PEDOT/A-CNTs//a-graphene asymmetric supercapacitor in volumetric unit.

The electrochemical performance of the asymmetric supercapacitor cell was further characterized by electrochemical impedance spectroscopy (EIS). Nyquist plot, as shown in **Figure 8(a)**, is achieved in the frequency range of 100 kHz–10 mHz of 5 mV applied voltage. It could be found that a semicircle in the high-frequency region and a sharp rise of the imaginary part of the electric impedance shown in the figure reflecting the dominance of the cell capacitance in the-low frequency region. As shown in the Nyquist plot, the semicircle at the middle/high frequency is due to the charge transfer resistance in the porous electrodes. The high-frequency intersection on the real axis of the Nyquist plot shown in the figure represents the internal resistances. Internal resistance of 0.1 Ω cm^2 of the cell is obtained in the figure when normalized with the area of the current collector of the capacitors indicating a high electrical conductivity and low ESR of the cells.

The maximum power density of the asymmetric supercapacitor cell is determined from Equation (4). **Figure 8(c)** presents the Ragone plot (gravimetric power density versus energy density) of the asymmetric supercapacitor derived from the galvanostatic discharge curves measured at different charge/discharge current densities following standard practice. In addition to gravimetric performance, the maximum power density is derived from Equation (3), where V is the operation voltage, which is 4 V here.

The volumetric energy and power densities are more important in practical applications. The cells exhibit both high volumetric and gravimetric power and energy density at 149 kW/L (233 kW/kg) and 113.2 Wh/L (176.6 Wh/kg), respectively. These values are significantly higher than those of other reported carbon-based symmetric supercapacitors, conducting polymer-based supercapacitors and other devices reported previously [8–10]. The pseudocapacitor nature of PEDOT has lower charge/discharge speed compared with that of the pure EDLC supercapacitors and hence the power density is lower than that of the A-aMEGO supercapacitors, which have been presented in the proceeding section.

In summary, an asymmetric supercapacitor, employing the conformal coating of PEDOT/A-CNT composite as one electrode and high density a-graphene flakes as the other electrode, has been developed in this paper. PEDOT/A-CNT composite combines fast ion transport pathways, enhances charge storage capability, and reduces ESR while a-graphene electrode fabricated from a self-assembly process, which possesses exceedingly high specific gravimetric and volumetric capacitance. The two electrodes are individually tailored to control the nanomorphology and work synergistically together in the asymmetric cell configuration. The ECW has been expended up to 4 V. Tailoring of the two electrodes materials at a scale approaching that of the ions can allow asymmetric supercapacitor performance to be further expanded to meet the requirement of a broad range of energy storage applications.

Acknowledgements

This work was supported by AFOSR under Grant no. FA9550-11-1-0192. Reproduced from Ref. [4] with permission from ELSEVIER. Reproduced from Ref. [6] with permission from the Royal Society of Chemistry.

Author details

Yue Zhou* and Qiming Zhang

*Address all correspondence to: yuezhou26@gmail.com

Department of Electrical Engineering, Pennsylvania State University, University Park, Pennsylvania, USA

References

[1] W. Lu, L. Qu, K. Henry, L. Dai. High performance electrochemical capacitors from aligned carbon nanotube electrodes and ionic liquid electrolytes. Journal of Power Sources. 2009;189(2):1270. DOI: 10.1016/j.jpowsour.2009.01.009

[2] C.L. Pint, N.W. Nicholas, S. Xu, Z. Sun, J.M. Tour, H.K. Schmidt, R.G. Gordon, R.H. Hauge. Three dimensional solid-state supercapacitors from aligned single-walled carbon nanotube array templates. Carbon. 2011;49(14):4890. DOI: 10.1016/j.carbon.2011.07.011

[3] D.N. Futaba, K. Hata, T. Yamada, T. Hiraoka, Y. Hayamizu, Y. Kakudate, O. Tanaike, H. Hatori, M. Yumura, S. Iijima. Shape-engineerable and highly densely packed single-walled carbon nanotubes and their application as super-capacitor electrodes. Nature Materials. 2006;5:987. DOI: 10.1038/nmat1782

[4] Y. Zhou, M. Ghaffari, M. Lin, E.M. Parsons, Y. Liu, B.L. Wardle, Q.M. Zhang. High volumetric electrochemical performance of ultra-high density aligned carbon nanotube supercapacitors with controlled nanomorphology. Electrochimica Acta. 2013;111:608. DOI: 10.1016/j.electacta.2013.08.032

[5] J. Lin, Y. Liu, Q.M. Zhang. Charge dynamics and bending actuation in Aquivion membrane swelled with ionic liquids. Polymer. 2011;52(2):540. DOI: 10.1016/j.polymer.2010.11.030

[6] Y. Zhou, N. Lachman, M. Ghaffari, H. Xu, D. Bhattacharya, P. Fattahi, M.R. Abidian, S. Wu, K.K. Gleason, B.L. Wardle, Q.M. Zhang. A high performance hybrid asymmetric supercapacitor via nano-scale morphology control of graphene, conducting polymer, and carbon nanotube electrodes. Journal of Materials Chemistry A. 2014;2:9964. DOI: 10.1039/c4ta01785d

[7] Y. Zhu, S. Murali, M.D. Stoller, K.J. Ganesh, W. Cai, P.J. Ferreira, A. Pirkle, R.M. Wallace, K.A. Cychosz, M. Thommes, D. Su, E.A. Stach, R.S. Ruoff. Carbon-based supercapacitors produced by activation of graphene. Science. 2011;332(6037):1537. DOI: 10.1126/science.1200770

[8] B.G. Choi, M.H. Yang, W.H. Hong, J.W. Choi, and Y.S. Huh. 3D macroporous graphene frameworks for supercapacitors with high energy and power densities. ACS Nano. 2012;6:4020. DOI: 10.1021/nn3003345

[9] A. Izadi-Najafabadi, S. Yasuda, K. Kobashi, T. Yamada, D.N. Futaba, H. Hatori, M. Yumura, S. Iijima, K. Hata. Extracting the full potential of single-walled carbon nanotubes as durable supercapacitor electrodes operable at 4 V with high power and energy density. Advanced Energy Materials. 2010;22:E235. DOI: 10.1002/adma.200904349

[10] Z. Chen, J. Wen, C. Yan, L. Rice, H. Sohn, M. Shen, M. Cai, B. Dunn, Y. Lu. High-performance supercapacitors based on hierarchically porous graphite particles. Advanced Energy Materials. 2011;1:551. DOI: 10.1002/aenm.201100114